Monitoring Active Filters under Automotive Aging Scenarios with Embedded Instrument

Jinbo Wan and Hans G. Kerkhoff
Testable Design and Testing of Integrated Systems Group
University of Twente, CTIT
Enschede, the Netherlands
j.wan@utwente.nl, h.g.kerkhoff@utwente.nl

***Abstract*—in automotive mixed-signal SoCs, the analogue/mixed-signal front-ends are of particular interest with regard to dependability. Because of the many electrical disturbances at the front-end, often (active) filters are being used. Due to the harsh environments, in some cases, degradation of these filters may be encountered during lifetime and hence false sensor information could be provided with potential fatal results. This paper investigates the influence of aging in three different types of active filters in an automotive environment, and presents an embedded instrument, which monitors this aging behaviour. The monitor can be used for flagging problems in the car console or initiate automatic correction.**

Keywords-component; active filters; testing; aging; monitoring; NBTI; embedded instruments

I. INTRODUCTION

With the introduction of new semiconductor technologies, as well as the increased usage of integrated heterogeneous circuits in safety-critical applications, dependability is getting increasingly important [1].

In order to prepare deep-submicron SoCs for safety-critical applications, the dependability of the SoCs, especially the analog/mixed-signal IP based SoCs, needs to be drastically improved. There are not many publications concerning the dependability of this type of SoCs. Most of the publications are dealing with *digital* IP-based SoCs and use for instance redundant components together with dynamic routing to improve the dependability [2].

An industrially important area for safety-critical SoC applications is the car electronics industry. There are currently many electronic systems improving the safety in cars, like ABS and EPS [3]. Especially with the introduction of hybrid cars, and future advanced car-control options (e.g. automatic radar-based car collision prevention) the safety levels of the required electronics have to be extremely high. The conditions (mission profile) under which these SoC electronics have to operate can be very harsh, upto 175^0C, including high moisture and vibrations, among others. A lifetime of 20 years for trucks has to be guaranteed.

978-3-9810801-8-6/DATE12/©2012 EDAA

This research has been conducted within the CATRENE project TOETS (CT-302) which is financially supported by Agentschap NL.

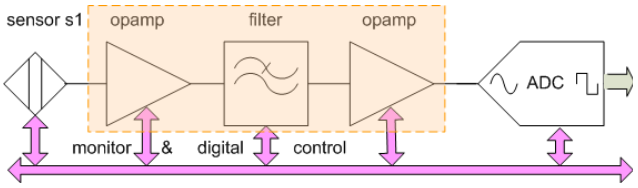

Figure 1. Possible analogue/mixed-signal front-end in cars

Especially the analogue/mixed-signal front-end (but also back-end) in cars is of interest, as the sensors (e.g. angular, temperature, pressure) and associated electronics, are often at close distance to the measured physical quantity.

A generic setup of car front-end electronics is shown in Fig.1. A sensor providing e.g. a small noisy voltage signal is first amplified, and subsequently filtered, and again amplified before entering an ADC for digitalization. Advanced systems can include some programmability for monitoring and calibration (purple). As self-monitoring and self-correcting opamps under aging have been discussed elsewhere [4], this paper will be focussed on (active) filters (Fig. 1). Incorrect filter transfer functions, e.g. in terms of amplitude, phase or cut-off frequency can seriously detoriate sensor data, and can hence endanger human life. As embedded instruments are more generic and wider to use, we have taken this path of aging monitoring in filters during lifetime. Process variations (at life-time zero), although of high importance, are not within the scope of this paper.

This paper is organized as follows. First aging models and aging experiments used in the paper are discussed. Then three types of active second-order low-pass (LP) filters are investigated in terms of their aging behaviour under harsh (automotive) conditions. They are an active-RC LP filter, a switched-capacitor LP filter and finally an OTA-C LP filter. The aging behaviour of the latter gives rise to the requirement of monitoring its behaviour over its lifetime.

Circuit-level simulations of this filter show that particular currents are well correlated with this behaviour and hence candidates for aging monitoring. Next, a current monitor is presented and shown to be suitable as embedded instrument for aging and communicating to the outside world via P1687 (IJTAG). Finally, some conclusions are being provided.

II. AGING MODELS USED IN AGING EXPERIMENTS

There are many aging effects in nanometer CMOS technologies, like hot carrier injection (HCI), time-dependent dielectric breakdown (TDDB), negative bias temperature instability (NBTI), and so on. Among them, NBTI is the most critical reliability threat [5]. Hence this paper will focus on the NBTI aging influence on active filters in 65nm CMOS technology.

Accurate measurement of the NBTI is difficult. This is because the NBTI degradation can recover after the stress is removed. And the recovering is really fast and hence requires ultra-fast measurement methods to avoid experimental artefacts associated with the common measure-stress-measure approach [6]. However, the measurement methods that have been proposed are still far from perfect. It is the same for NBTI modelling. In fact there is no single NBTI model that can perfect explain all phenomena found by stress measurements until now [6].

Among the NBTI models proposed, three groups are very popular. They are power models (PM) [7], reaction-diffusion models (RD) [8] and hole-trapping models (HT) [5]. The PM models are based on function fitting and carry out extrapolation from DC stress measurements. They can work well in DC stress situations. However, it is prove to be too optimistic for AC stresses [5]. As an improvement, RD models and HT models can both model the recovering effect of the NBTI, and can model the AC stress much better. Yet they are still competing with each other for usefulness [6].

In this paper, we use Cadence Relxpert to simulate the NBTI degradation on active-filters. Only threshold voltage degradation for PMOS transistors are considered. The NBTI model used in Relxpert is a PM model, which can be written as the expression in (1).

$$\Delta V_{TH}(t_{stress}) = A \cdot exp(\gamma V_{stress}) exp\left(-\frac{E_a}{kT}\right) t_{stress}^{n} \quad (1)$$

Where ΔV_{TH}, V_{stress}, T, k and t_{stress} are threshold degradation of the PMOS transistor, the applied stress voltage, the temperature, Boltzmann constant and the stressed time. The fitting parameters are A, γ and E_a, which need to be extracted from stress measurements.

There are two reasons to use the PM model based NBTI simulation here. First, most foundries can only provide the PM model parameters based on (1) for the NBTI degradation in their CMOS technologies. Second, one wants to verify the worst-case scenario. That often means the maximum possible DC stresses instead of AC stresses. For example, the inputs of the active-filters are biased at a DC level closed to ground for the worst case scenario, since the input differential pairs in all active-filters are PMOS. At a later stage of research a more accurate model (including charge restoration and stochastic) will be used. The reliability behaviour of the passive components in the filters is part of the used design kit. On-chip resistor and capacitor aging behaviour have been studied in the past [9][10].

All NBTI aging simulations have been done for a mission profile of 20 years, at 200℃. All circuits were designed in Cadence in a 65nm CMOS process with 1.2V power supply.

III. AGING EXPERIMENTS ON ACTIVE FILTERS

A. Active filters

In the past, we have carried out many aging simulations on CMOS circuits in automotive SoCs, such as automotive CAN IPs [11] and OpAmps [4]. Especially the latter has aided our simulations for active filters, as weak spots in their OpAmps under specific operating conditions were known.

Three kinds of second-order Butterworth low pass filters have been designed. They are respectively an Active-RC LP filter, switched-capacitor (SC) LP filter and an OTA-C LP filter. All these LP filters have the same -3dB cutoff frequency being 1 KHz. The DC gains of the LP filters are approximately 0dB.

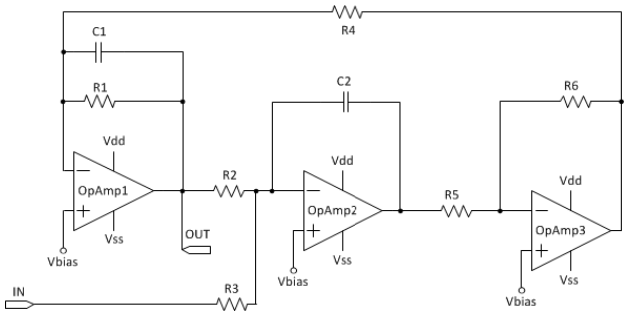

Figure 2. Circuit design of the Active-RC LP filter

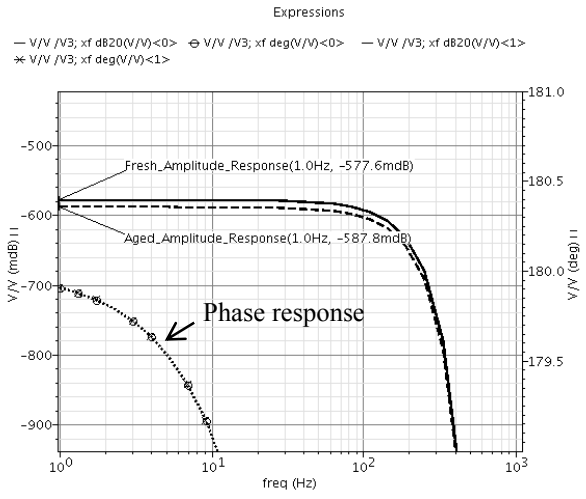

Figure 3. Simulated transfer function of a fresh active-RC LP filter circuit and after NBTI aging

B. Active-RC LP filter

As first filter, an active RC low-pass filter has been investigated. The circuit diagram in 65nm CMOS is shown in Fig. 2. It uses the Tow–Thomas universal biquad structure [12]. The design employs three operational amplifiers, which are using a PMOS input differential pair with a rail-to-rail class-AB output stage, providing more than 40 dB gain. The Vbias in Fig. 2 is a DC voltage for input biasing.

Fig. 3 shows that NBTI is not a problem for the active RC low-pass filter, as NBTI has nearly no effect on the designed Active-RC LP filter. Especially the phase behaviour shows no difference. The explanations for this dependable behaviour are following. First, the frequency behaviour is mostly determined by the passive RC components. They are insensitive to NBTI aging (unless MOS capacitors). Second, the feedback reduces the sensitivity to the gain of the Opamps if the loop gain is high. So the gain degradation of the Opamps does not cause the filter performance degradation. What's more, the filter DC gain is low (0db). Thus the offset caused by the NBTI is not a problem. Hence in this case there is no need for monitoring this filter on its aging behaviour during life time.

C. Switched-Capacitor LP Filter

As second filter, a switched-capacitor second-order low-pass filter has been investigated. The circuit diagram is shown in Fig. 4. It employs the Fleischer-Laker approach [13]. The used operational amplifiers are the same as before, a PMOS input differential pair with a rail-to-rail class-AB output stage.

Fig. 5 indicates that NBTI has nearly no effect, and hence aging is also not a problem. The design was not optimized in terms of reducing the overshoot, but note that in order to visualize the aging effects, the horizontal scale was made very small. In the case of the phase, the difference is not even visible. Therefore, also in this case no embedded instrument is required to monitor the aging behaviour of the filter.

The explanations for this dependable behavior are similar to the Active-RC filter. The frequency behavior is determined by the capacitors and the clock period, and the feedback reduces the sensitivity to the gain of the Opamps if the loop gain is high.

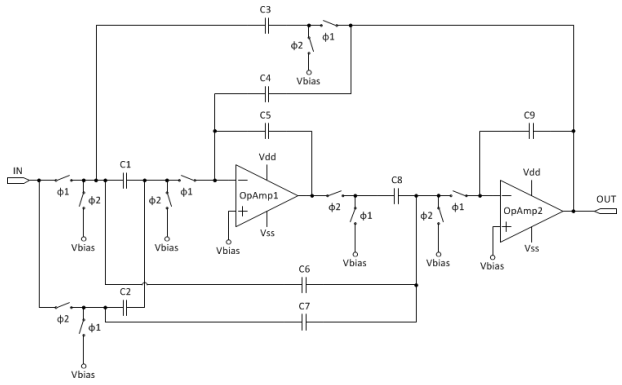

Figure 4. Circuit design of the second-order switched-capacitor LP filter

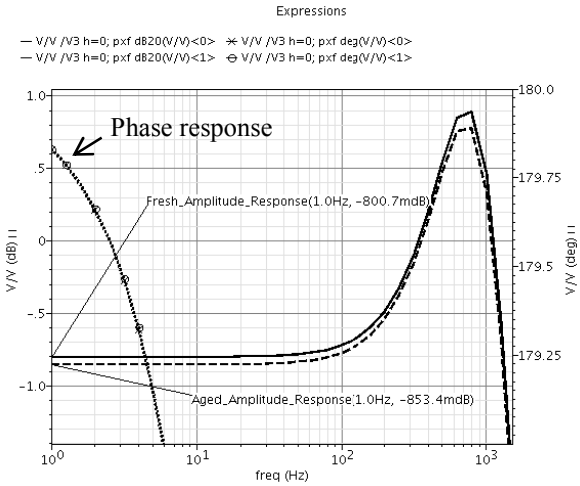

Figure 5. Simulated transfer function of fresh switched-capacitor second-order LP filter circuit and after NBTI aging

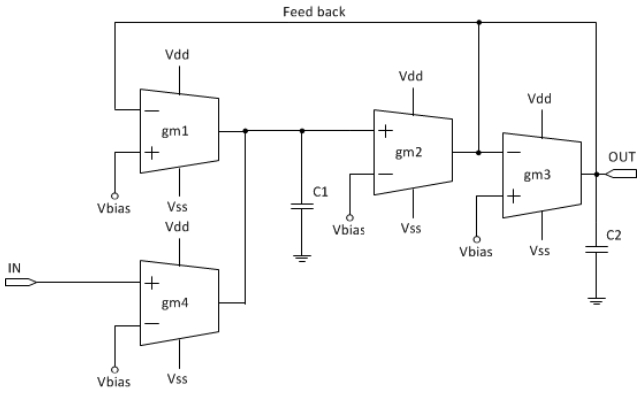

Figure 6. Circuit design of the second-order OTA-C LP filter

D. OTA-C LP filter

As last example of a filter, an OTA-C LP filter has been investigated. Again, the Tow–Thomas universal biquad structure has been used [18]. The OTAs use a PMOS input differential pair with current mirror output. The design is shown in Fig. 6.

Fig. 7 shows the simulated aging behaviour. One can observe, that the filter frequency has changed as is the phase in the case of aging. The reason can be found by investigating the transfer function of the OTA-C filter, which is shown in (2).

$$H(s) = \frac{V_{OUT}}{V_{IN}} = \frac{{g_{m2}g_{m4}}/{C_1C_2}}{s^2+\left({g_{m3}}/{C_2}\right)s+{g_{m1}g_{m2}}/{C_1C_2}} \quad (2)$$

$$\omega_{-3dB} = \sqrt{\frac{g_{m1}g_{m2}}{C_1C_2}} \quad (3)$$

$$H(0) = \frac{g_{m4}}{g_{m1}} \quad (4)$$

From the transfer function, the -3dB frequency and the DC gain of the filter can be expressed as in (3) and (4). They show that the -3dB frequency is determined not only by the capacitors, but also by the multiplication of two trans-conductances. And the DC gain is determined by the ratio of two trans-conductances.

The NBTI effect can increase the thresholds of the PMOS transistors in the input differential pair. The drain currents will be degraded and hence the trans-conductance of the OTA will be reduced after aging. An interesting result found by simulations shows that the trans-conductance degradation for all OTAs in the filter are in close correlation. This is because the stresses for each OTA are proportional and influenced by the overall input signal of the filter. So the $H(0)$ will be relatively aging insensitive (4) and ω_{-3dB} will be more sensitive to the aging (3).

This filter could be a candidate for aging observation via an embedded instrument. One option could be to just monitor the output and compare with a "correct" referenced output, like the method shown in [14]. However, the approach used in [14] cannot monitor the aging degradation, because the reference circuits are also aged. Another option could be concurrent error detection [15][16]. However, the concurrent detection method also faces the same problem. The error detection circuits are aged as well, which may cause false alarms or miss alarms.

It is possible to investigate if there is already an internal signal in the filter that shows a high correlation with the aging behaviour, thereby easing the design of an embedded instrument. During simulation we have observed a number of signals in the filter that might have that property. It turned out, the current in the differential pair transistors of the OTA is an excellent candidate. This is supported by the correlation graph shown in Fig. 8. It shows the -3dB frequency versus the DC cascode current. Each star represents another year of aging, which indicates that the largest variation in the -3dB frequency is in the first year. Actually, this approach can be considered as a sensitivity analysis for the aging behaviour.

This has supported the conclusion, that a suitable current sensor would be a good embedded instrument to monitor the aging. In fact there are already some IDDQ monitors which could measure the current flowing in the differential pair [17][18]. However, the IDDQ monitor often requires a high power supply voltage which is harmful for reliability, and the circuits are complex. So in the next section, a much simpler current monitor with standard supply voltage will be presented.

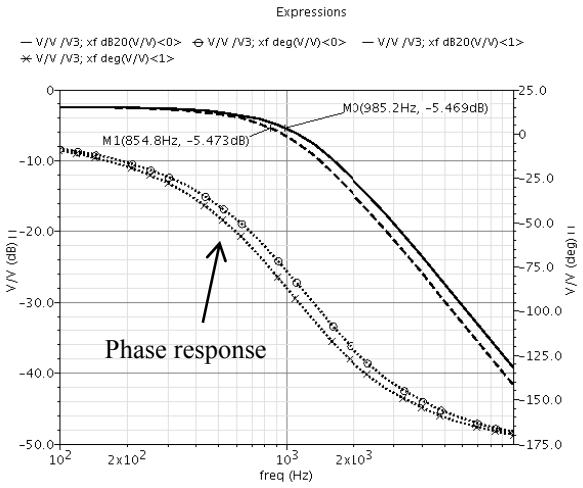

Figure 7. Simulated transfer function of fresh second-order OTA-C LP filter circuit and after NBTI aging

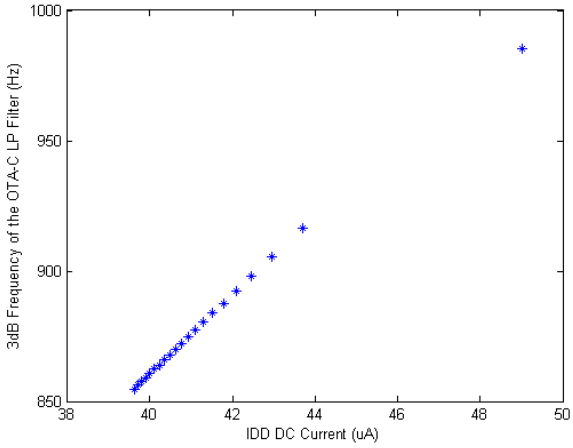

Figure 8. Simulated monitor current versus 3dB frequency transfer characteristic diagram aging

IV. MONITORING THE BEHAVIOUR VIA AN EMBEDDED INSTRUMENT

In this section a very simple aging monitor is presented, basically measuring the differential pair transistor current in the first stage at DC operational points. The correlation is indicated as well as the possible alarm function that can be used for either flagging in the car console, or correction.

A. Embedded instrument for monitoring the 3dB frequency shift resulting from aging.

A configuration for the aging monitor embedded instrument is shown in fig. 9. The current monitor takes the same input stress as the filter. Hence it will suffer the similar stress as the first OTA stage in the filter. The monitor will compare the current it sensed with an reference current, and give the aging

alarm signal when there is too much difference. The aging monitor can work both on-line and off-line.

Although the embedded aging-monitor instrument is working under the P1687 format (and potentially under IEEE 1149.4), the embedded monitor communicates with the outside world by digital signals only. For simplicity, the digital interfacing circuit is not shown here.

A digital signal can set the reference current via a programmable current source or a current-steering DAC, providing at some moment a digital signal if this level (aging setting) is reached. This makes the instrument very easy to use. The digital signals can be internally or externally provided, but also by an embedded processor.

The circuit design of the monitor circuit is shown in Fig. 10. It is a very simple circuit, in 65 nm CMOS processing. A pseudo differential transistor pair with diode connected transistor loads is used to sensor the similar current through the differential pair transistors in the first stage of the OTAs. A current-mirror based current comparator compares the sensed current and a reference current. The *Aging_alarm* signal is produced to indicate the occurrence of a certain amount of performance degradation due to aging.

The NBTI degradation of the monitor circuits is considered in the simulation as well. However, the reference current is assumed to be aging insensitive. It is reasonable if the reference current is directly provided externally. While, if the reference current comes from a programmable current source or a DAC, the aging of these circuits also need to be considered. These works are under research together with a new NBTI model for arbitrary-waveform stresses in our group.

Fig. 11 shows the reference current value versus *Aging_alarm* pin voltage. If the reference current is low, the *Aging_alarm* voltage will be high, or in digital, one. If the reference current is high, the *Aging_alarm* voltage will be low, or in digital, zero. A reference current threshold value could decide the *Aging_alarm* pin voltage to be zero or one. The

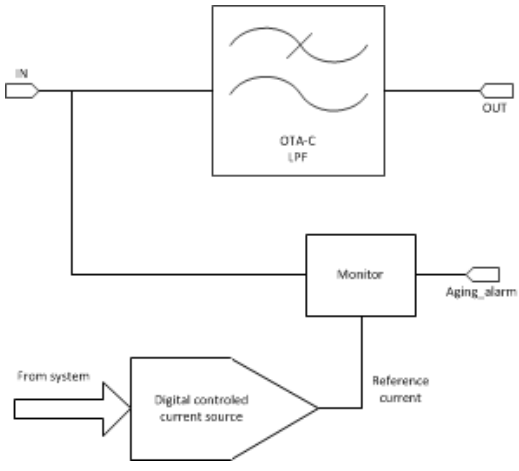

Figure 9. Proposed configuration of a embedded instrument for monitoring the aging

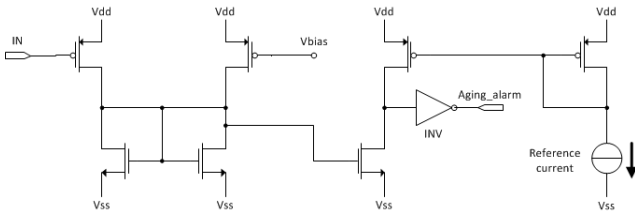

Figure 10. Circuit design of the embedded current monitor

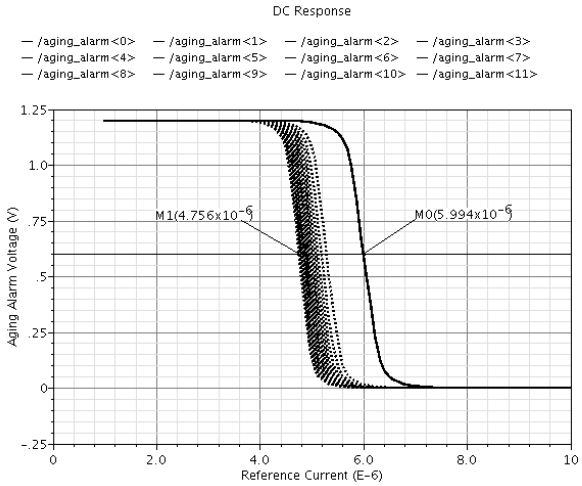

Figure 11. Aging alarm in voltage versus the reference current

threshold current value is selected as the real reference value during the self-calibration after fabrication. Finally, Fig. 12 shows the good correlation of the measured current with (changing) 3dB frequency.

From this figure, one can see the threshold current value is smaller with aging. That could be used to detect the aging. For example, based on the figure, we select 5uA as the real reference current. In fresh state, the *Aging_alarm* signal is zero. When aging for around 6 years, the aging alarm signal will be one, which means 10% degradation occurred.

Since the aging-monitor instrument needs to detect 1μA current drop, we have used a programmable current source with steps of 0.1μA. Furthermore, to cover the PVT variation, the programmable current source should cover 10 μA in range. This means it requires a 6 to 7 bits digital programmable current source or current-steering DAC. The design can be similar to the one used to monitor offsets in OpAmps [4].

V. CONCLUSIONS

This paper has dealt with monitoring the aging process of active filters in automotive analogue front-ends in SoCs by using an embedded instrument. We have shown by experiments that the feed-back in many active filters provide sufficient protection against aging scenarios in analogue front-ends even under harsh automotive mission profiles.

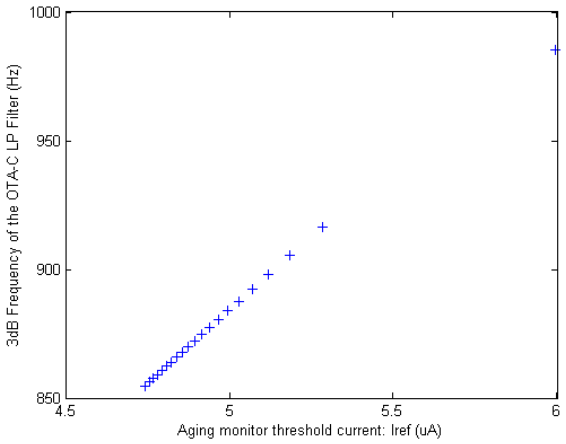

Figure 12. Correlation of the aging embedded instrument with filter

However in some cases, like the second-order OTA-C low-pass filter example in this paper, indeed filter characteristics may change to the extend to endanger sensor readings. This can potentially endanger the car safety. By monitoring the filter during lifetime using an embedded instrument, either car console flagging or direct corrective actions can be taken.

Finally, we have shown the design of an aging-monitor in the same process as the filter, and also validated its capabilities, enabling a highly dependable analog/mixed-signal front-end. The aging monitor is generic in its nature, and can hence also be used for other IPs.

ACKNOWLEDGMENT

The authors like to acknowledge the fruitful discussions with H. Manhaeve of QStar Technologies, and G. Smit, A. Kokkeler, M. Bekooij and B. Molenkamp of CAES.

REFERENCES

[1] P. Chaparala, D. Brisbin, J. Kim, and B. OConnell, "Reliability challenges in analog and mixed signal technologies," in *2007 14th International Symposium on the Physical and Failure Analysis of Integrated Circuits*, 2007, pp. 135-140.

[2] H. G. Kerkhoff and X. Zhang, "Design of an infrastructural IP dependability manager for a dependable reconfigurable many-core processor," in *2010 Fifth IEEE International Symposium on Electronic Design, Test & Applications*, 2010, pp. 270-275.

[3] J. Guo, L. Chu, H. Liu, M. Shang, and Y. Fang, "Integrated control of active front steering and electronic stability program," in *2010 2nd International Conference on Advanced Computer Control*, 2010, pp. 449-453.

[4] J. Wan and H. G. Kerkhoff, "Boosted gain programmable opamp with embedded gain monitor," in *International SoC Design Conference*, 2011, pp. 1-4, in press.

[5] E. Maricau, L. Zhang, J. Franco, P. Roussel, G. Groeseneken, and G. Gielen, "A compact NBTI model for accurate analog integrated circuit reliability simulation," in *2011 Proceedings of the European Solid-State Device Research Conference (ESSDERC)*, 2011, vol. 10, pp. 147-150.

[6] S. Mahapatra et al., "A critical re-evaluation of the usefulness of R-D framework in predicting NBTI stress and recovery," in *2011 International Reliability Physics Symposium*, 2011, pp. 6A.3.1-6A.3.10.

[7] M. Kole, "Circuit realiability simulation based on Verilog-A," in *2007 IEEE International Behavioral Modeling and Simulation Workshop*, 2007, pp. 58-63.

[8] M. ALAM and S. MAHAPATRA, "A comprehensive model of PMOS NBTI degradation," *Microelectronics Reliability*, vol. 45, no. 1, pp. 71-81, Jan. 2005.

[9] "Chip resistor reliability test data." [Online]. Available: http://www.venkel.com.

[10] "Quality and reliability data," *Application note AN-0004*. [Online]. Available: http://www.syfer.com.

[11] V. Kerzérho and H. G. Kerkhoff, "The search for resilience weak spots in automotive mixed-signal circuits," in *2011 IEEE 17th International Mixed-Signals, Sensors and Systems Test Workshop (IMS3TW)*, 2011, pp. 1-6, in press.

[12] P. E. Fleischer and K. R. Laker, "A family of active switched-capacitor biquad building blocks," *The Bel System Technical Journal*, vol. 58, no. 10, pp. 2235-2269, 1979.

[13] L. Thomas, "The biquad: part II--a multipurpose active filtering system," *IEEE Transactions on Circuit Theory*, vol. 18, no. 3, pp. 358-361, 1971.

[14] J. L. Huertas, A. Rueda, and D. Vazquez, "Testable switched-capacitor filters," *IEEE Journal of Solid-State Circuits*, vol. 28, no. 7, pp. 719-724, Jul. 1993.

[15] A. Chatterjee, "Concurrent error detection and fault-tolerance in linear analog circuits using continuous checksums," *IEEE Transactions on Very Large Scale Integration (VLSI) Systems*, vol. 1, no. 2, pp. 138-150, Jun. 1993.

[16] H.-G. D. Stratigopoulos and Y. Makris, "Concurrent detection of erroneous responses in linear analog circuits," *IEEE Transactions on Computer-Aided Design of Integrated Circuits and Systems*, vol. 25, no. 5, pp. 878-891, May 2006.

[17] R. Rajsuman, "Iddq testing for CMOS VLSI," in *Proceedings of the IEEE*, 2000, vol. 88, no. 4, pp. 544-568.

[18] S. R. Mallarapu and A. J. Hoffman, "Iddq testing on a custom automotive IC," *IEEE Journal of Solid-State Circuits*, vol. 30, no. 3, pp. 295-299, Mar. 1995.